Original Article Clinics in Orthopedic Surgery 2026;18:366-374 • https://doi.org/10.4055/cios25232

Can the Finite Element Method Be Applied to Patient-Specific Implant Evaluation?

Suyeon Lee, MSc*, Hyenmin Park, BSc†, Hyun Guy Kang, MD*,‡, June Hyuk Kim, MD‡, Im Doo Jung, PhD§, Jong Woong Park, MD†,‡

*Medical Engineering Branch, Division of Technology Convergence, National Cancer Center, Goyang,
†Surgical Oncology Branch, Division of Clinical Research, National Cancer Center, Goyang,
‡Orthopaedic Oncology Clinic, Center for Sarcoma, National Cancer Center, Goyang,
§Department of Mechanical Engineering, Ulsan National Institute of Science and Technology, Ulsan, Korea

Background: The introduction of 3-dimensional printing has revolutionized orthopedic surgery, enabling patient-customized implants to address complex bone defects. However, ensuring reliable fixation remains a considerable challenge. Herein, we developed a finite element analysis (FEA)-based flow designed to evaluate implant fixation across various anatomical sites.

Methods: We applied this flow to the pelvic region to validate its fixation strategies and optimize the design across different osteointegration stages: acute, pre-, and post-osteointegration. Effects of screw-fixation methods (short screws in the cancellous bone and long screws in the cortical bone) on patient outcomes were analyzed and validated using data from 2 patients.

Results: Predictive outcomes aligned closely with clinical results in terms of the location and timing of screw-fixation failure.

Conclusions: The study findings affirm the potential of FEA to verify implant design and fixation strategies and to enhance surgical success rates through improved preoperative planning.

Keywords: *Orthopedics, Three-dimensional printing, Implant, Bone reconstruction, Finite element analysis*

In orthopedics, 3-dimensional (3D) printed implants have revolutionized reconstructive surgeries, particularly for treating complex cortical bone defects.[1-6] These implants are customized to fit individual patient anatomies and are particularly useful for pediatric patients with small bones or for oncology patients in whom tumor implants cannot be used, such as in patients requiring pelvic reconstructions.[7,8] In addition, 3D customized implants can preserve the original joint when a tumor is located near the joint but has not invaded it.[9] Durable fixation is an important factor for successful bone reconstruction using implants. Owing to the customized nature of individual implants, implant design, and fixation methods must be validated each time, considering the individual patients' anatomical differences, bone quality, location and shape of the bone defect, and especially the remaining cortical bone to be screwed in.[10]

However, sufficient time cannot be devoted to evaluating tumor implants owing to the tumor progression. In this situation, finite element analysis (FEA) can be a useful tool to efficiently evaluate implants instead of mechanical experiments.[11-15] FEA has been used in most previous studies to observe the stress distribution of the customized 3D-printed implant or identify structural weaknesses, assuming that the implant is fully bonded to the remaining bone.[11,16] However, in analyzing customized implants, it is important to analyze the implant after osteointegration and predict whether it can be sufficiently stabilized until it fully bonds with the remaining bone. Inadequate fixation can result in screw pull-out or fracture of fixation or im-

Received June 27, 2025; Revised October 14, 2025;
Accepted October 16, 2025
Correspondence to: Jong Woong Park, MD
Orthopaedic Oncology Clinic, Center for Sarcoma, Research Institute and Hospital, Graduate School of Cancer Science and Policy, National Cancer Center, 323 Ilsan-ro, Ilsandong-gu, Goyang 10408, Korea
Tel: +82-31-920-1664, Fax: +82-31-920-2798
E-mail: jwpark82@ncc.re.kr
Suyeon Lee and Hyenmin Park contributed equally to this work.

plants before complete integration with the host bone tissue.[17,18] Therefore, a comprehensive analysis of all phases is necessary, considering the clinical situation before and after osteointegration onto the implant surface.

We introduced an FEA approach designed for use across multiple anatomical regions to address the challenges of implant validation. In this study, we applied the FEA approach to one of the most complex regions, the pelvis, to assess its predictive accuracy in reconstructive surgery using patient-customized 3D-printed implants. Representative cases of patients with 3D-printed implants were selected, and a comprehensive FEA was conducted under clinical boundary conditions across different recovery phases to evaluate the alignment of the predictions with the clinical outcomes.

METHODS

The study was approved by the Institutional Review Board of National Cancer Center (IRB No. 2017-0129) and conducted in accordance with relevant guidelines and regulations including the Declaration of Helsinki. Written informed consent was obtained from all patients prior to their participation in the study.

Patient Information

To ascertain the use of FEA in validating the design of customized orthopedic implants, individuals meeting the following criteria were carefully selected. First, the candidate was required to have undergone a minimum follow-up period of 3 years. Second, the implant under consideration was required to have adequate dimensions and to exhibit a complex geometric configuration. Third, patients were required to have favorable bone quality to allow the simplification of boundary conditions in the finite element model. Limb-salvage surgery using 3D-printed implants is generally performed in relatively young, active patients without metastases and with expected long-term survival after tumor removal; thus, the bone quality of such patients is typically good, which justified this simplification. For this preliminary, proof-of-concept study, we intentionally selected cases wherein an implant-related adverse event occurred in either the acute or chronic postoperative phase to evaluate whether the proposed FEA workflow could identify the biomechanical risk factors associated with those events. Patients who underwent reconstruction using 3D-printed implants without implant-related adverse events were not included in this study. Finally, to assess the predictive accuracy of the FEA approach, we included only cases with sufficient imaging and clinical documentation to construct patient-specific finite element models.

We selected 2 patients using the criteria mentioned above. The first patient was a 64-year-old woman who was previously healthy and had good bone quality without osteoporosis. She was diagnosed with chondrosarcoma of the entire right pelvis (Fig. 1). The second patient was a 19-year-old active male patient with osteosarcoma affecting the entire right pelvis (Fig. 2). Both patients underwent major bone reconstruction using a 3D-printed Ti6Al4V customized implant with hip joint arthroplasty after type I, II, or III internal hemipelvectomies. Notably, the sacral cortex of the affected side was removed to achieve a wide skeletal margin. For clinical reasons, the implant had complex shapes with solid and lattice structures. The im-

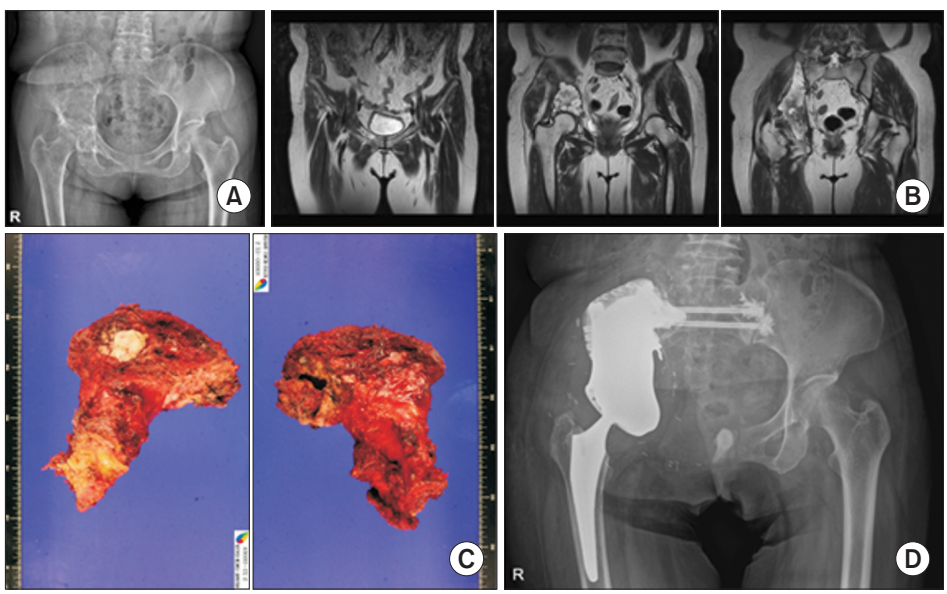

Fig. 1. Clinical images for case 1. Preoperative x-ray (A), magnetic resonance images (B), photographs of resected tumor (C), and postoperative x-ray (D).

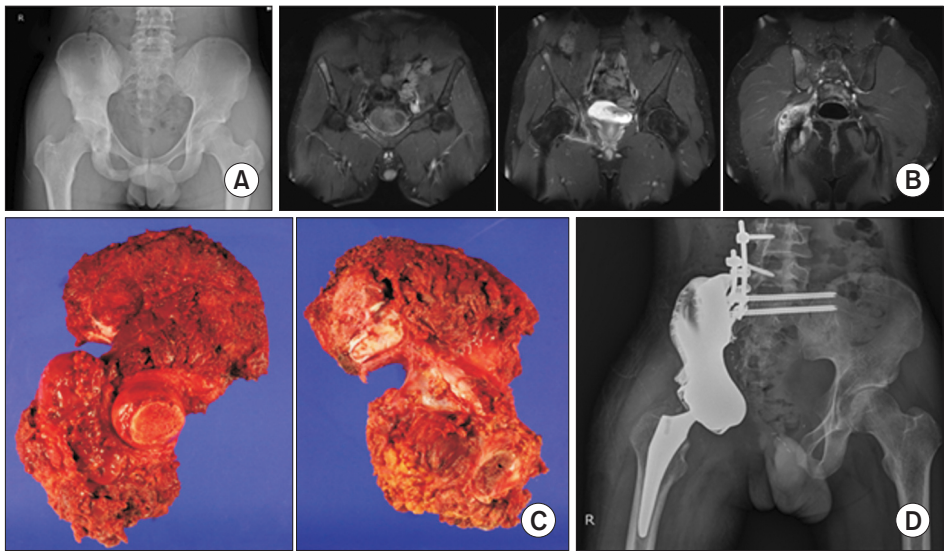

Fig. 2. Clinical images for case 2. Preoperative x-ray (A), magnetic resonance images (B), photographs of resected tumor (C), and postoperative x-ray (D).

plant body consisted primarily of a solid to bear the body weight. The sciatic notch was enlarged from the patient's original bone shape and the surface was treated to make it as smooth as possible for the neurovascular structures. Furthermore, the area interfacing with the sacrum bone was printed with a lattice structure featuring a 2 mm unit size to promote osteointegration, facilitating the creation of artificial porosity to foster a porous architecture.

Fixation was planned with 2 short screws in the first patient because the original surgical plan was disarticulation from the sacroiliac joint while preserving the sacral cortex. However, the sacral cortex of the affected pelvic bone was difficult to preserve, and sacral cancellous bone was revealed after bone tumor removal with a wide bone margin. The initial attempt to fix the screws using 2 short screws failed, and the short screws were replaced with long screws for bone-cement augmentation. In the second patient, surgical fixation involved inserting 2 long screws extending from the implant toward the contralateral pelvic bone, supplemented with spinal screws and a connecting rod for additional reinforcement. At 6 months postoperatively, the patient regained gait functionality without the need for assistive devices. However, at 27 months postoperatively, we observed fatigue-induced breakage in the upper long screw, followed by a fracture of the lower long screw at 33 months postoperatively.

Finite Element Model

The pelvic structures of both patients were modeled with finite element modeling using ANSYS SpaceClaim 2023 R2 (ANSYS Inc.) based on the stereolithography files converted from the digital imaging and communications in medicine images. Notably, each model included the sacrum, left pelvis, right pelvic implant, and pelvic surgical screw. In addition, the model included vertebral and spinal implant fixation screws in the second case, in which spinal fixation was also performed. The screws were aligned according to standard surgical practice, assuming complete locking at the insertion points.

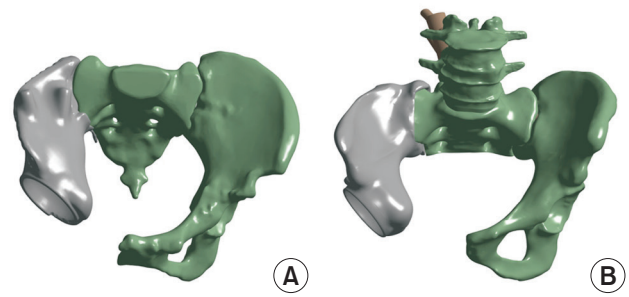

Fig. 3. Pelvic bone modeling for case 1 (A) and case 2 (B).

The analysis focused on optimizing the fixation method for the screws, omitting factors that did not have a significant impact on the results, and simplifying some of the structures to reduce unnecessary computational efforts. For example, the screws were modeled as cylindrical components without threads to prioritize stress analysis over geometric details. In addition, the small holes and lattice surfaces of the pelvic implants were not included in the model. However, the cortical and cancellous bones were modeled separately to accurately represent the bone's biomechanical behavior, with a 2-mm thickness assigned to the cortical bone based on the patients' computed tomography data (Fig. 3).

The mesh strategy was designed carefully to increase the model's accuracy and computational efficiency.

The sacrum and left pelvis were meshed using first-order elements without mid-nodes to ensure a simple yet effective representation of these complex anatomical structures. Except for the pedicle screws modeled with hexahedral elements, all other parts were represented by tetrahedral elements. The mesh size ranged from 1 to 5 mm and was determined using the force convergence criterion. Cortical and cancellous bones were integrated into a single part through shared nodes to ensure continuity between the 2 materials. Table 1 lists the properties of the materials[19-21] used in the simulation. We selected the bones and Ti-6Al-4V alloy to fabricate the implants and screws (Table 1).

Finite Element Analysis

FEA was conducted using ANSYS Workbench (ANSYS Inc.) to simulate the biomechanical behavior of the pelvic implants and screws under compressive loads. Assuming that the patients weighed 65 kg and 100 kg, respectively, compressive loads of 650 N and 1,000 N were applied to the model as normal forces. The contact conditions of the analytical models were distinctly defined to accurately assess the real biomechanical interactions according to the postoperative recovery phases: non-osteointegration and osteointegration phases. Fig. 4 shows the flowchart outlining the analysis process.

Non-osteointegration phase

In the non-osteointegration phase immediately after surgery, no direct bond formed between the implant and the bone, and implant fixation relied solely on screws. During this phase, the risk of screw pull-out due to bone wear or fracture from screw fatigue can be substantial. Therefore, complete fixation of the screws within the implant and the sacrum was assumed, and the contact conditions between the implant-screw and screw-sacrum were set to "bonded." We applied "frictionless" contact, allowing potential slip in the tangential direction to assess the risks associated with pelvic fixation screw pull-out and screw fatigue failure, to address the potential gaps between the implant and bone.

Screw pull-out

The von Mises stresses of the screwed bone were compared with the yield strength to analyze the possibility of screw pull-out (Table 2). This comparison was conducted

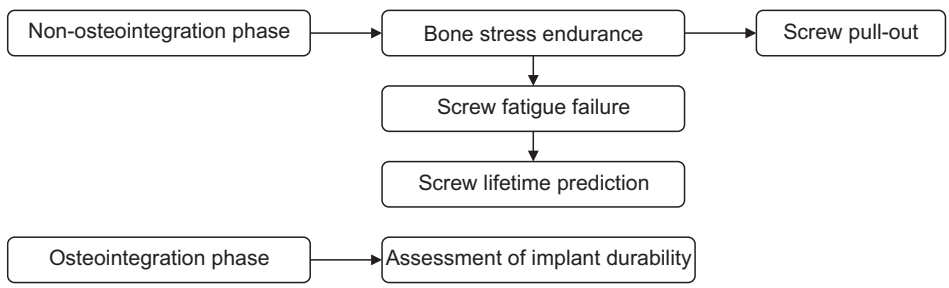

Fig. 4. Flowchart of finite element analysis.

Table 1. Material Properties Used in the Finite Element Simulation[19-21]

Material	Density	Young's modulus (MPa)	Poisson's ratio	Tensile strength (MPa)	Yield strength (MPa)
Cortical bone	1.64	16,700	0.26	106	105
Cancellous bone	0.16	155	0.30	6	1.95
Ti-6Al-4V	4.62	96,000	0.36	1,070	1,070

Table 2. Summary of Finite Element Analysis Results

Phase	Case	Screw fixed bone (MPa)	Implant (MPa)	Pelvic screw (MPa)
Non-osteointegration	I	17.7	499.2	485.1
	II	39.2	146.0	441.0
Osteointegration	II	14.7	12.6	49.9

considering the bone type (cortical or cancellous) that is most securely engaged, depending on the specific case. If the stress exceeded the yield strength, it indicated a pull-out scenario that could result in bone crushing and wear. Consequently, models identified as being at risk of screw pull-out are no longer considered for fatigue failure analysis of screws, as progression to fatigue fracture becomes impractical once screw dislodgement occurs.

Screw fatigue failure

In scenarios where screw pull-out does not occur, it is crucial to evaluate the endurance limit of the screws, specifically the duration they can withstand before bond forms between the implant and the bone. This evaluation includes assessing the potential for fatigue failure and predicting the fatigue lifetime using the S-N curve and Palmgren–Miner's rule, a cumulative damage model. The S-N curve plots the stress amplitude against the number of cycles to failure and was used in conjunction with Basquin's law (Eq. 1) to quantitatively assess screw performance under repeated loading. The S-N curve data were obtained from 3-point bending tests on Ti-6Al-4V alloy.[22]

$$\sigma_a = \sigma_f'(2N_f)^b \quad \text{(Eq. 1)}$$

, where σ_a is the stress amplitude under cyclic loading, σ_f' is the fatigue strength coefficient, Nf is the number of cycles to failure, and b is the fatigue strength exponent.

The fatigue life was predicted using the Palmgren–Miner's rule (Eq. 2).[23]

$$D = \sum_{i=1}^{k} \frac{n_i}{N_i} \quad \text{(Eq. 2)}$$

where "Ni" represents the number of cycles to failure as obtained from the S-N curve data, and "ni" quantifies the actual number of loading cycles the screw is to experience and is considered equivalent to the number of steps a patient takes daily. The pelvic screw connecting the implant and sacrum is predicted to fracture when the damage sum "D" reaches 1, using Miner's rule.

Daily cycle counts were estimated using a linear regression equation based on daily load cycles as a function of age and a pedometer that measured daily walking activities in normal subjects and patients with total hip arthroplasty (THA).[24] The mean age value was calculated between the age at surgery and the age at which the screw fracture was experienced and then applied to the linear regression equation to obtain more specific and appropriate age values. In addition, the daily walking cycles of the THA and normal walking periods were differentiated based on the time before and after the patient could perform normal activity, as documented in the patient records.

Osteointegration Phase

Once complete osteointegration is achieved, the contact condition is updated to "Bonded," which signifies a fully integrated state between the implant and bone. This phase represents a long-term scenario in which the implant and the bone function as a single unit and provide high stability. In this phase, the analysis is focused on evaluating the durability of the implant structure under a continuous load, ensuring that no significant stress or deformation results in failure. This analysis aimed to provide a comprehensive assessment of stress distribution and identify potential vulnerabilities within the implant system, thereby ensuring its reliability for sustained clinical performance.

RESULTS

Case 1: Non-osteointegration Phase

The simulation results for the first patient revealed a maximum von Mises stress of 499.24 MPa on the implant and 485.14 MPa on the pelvic screws securing the implant (Fig. 5). However, the stress on the cancellous bone region, where the short screw was anchored was 17.46 MPa (Fig.

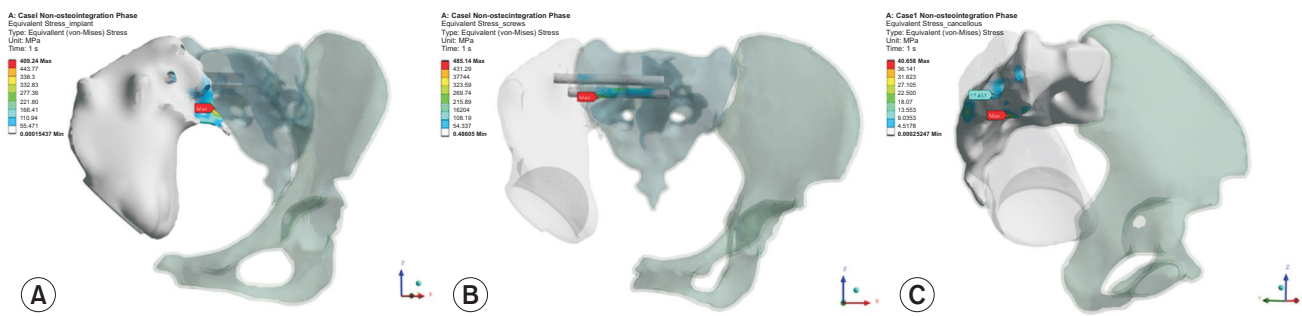

Fig. 5. Von Mises (VM) stress for case 1 during the non-osteointegration phase. VM stress of the pelvic implant (A), main screws (B), and cancellous bone around the main screws (C).

5), which was significantly higher than the yield strength of the cancellous bone (Table 1), indicating a high probability of screw pull-out due to wear of the cancellous bone. Therefore, further analysis of screw fatigue life and the osteointegration phase was not performed for this patient because of the predicted risk of screw pull-out. During the actual surgery, an attempt was made to fix the pelvic implant with short screws, but it resulted in the anticipated screw pull-out. Consequently, it was necessary to replace the screws with longer screws anchored to the opposite side of the cortical bone.

Case 2: Non-osteointegration Phase

The simulation results for the second patient showed that the maximum Von Mises stress on the implant was 146 MPa, and 441 MPa for the pelvic screw connecting the implant to the left pelvis and penetrating the sacrum (Fig. 6A and B). The pelvic screw anchoring in the cortical bone of the left pelvis experienced stress of approximately 39.2 MPa (Fig. 6C), which was safely below the cortical bone yield strength, indicating a minimal risk of bone damage or wear that could lead to screw pull-out. Given the low likelihood of pull-out, this study's focus shifted to evaluating the fatigue life of the pelvic screws under repetitive compressive loads. For the first 6 months postoperatively, the patient maintained a relatively low activity level, used crutches, and moved cautiously. Daily gait cycles during this period were calculated based on the linear regression analysis of patients with THA, with an average of approximately 6,659 cycles daily. As the patient's activity level gradually returned to normal with typical college life, this number was expected to increase to 14,488 cycles daily, reflecting the gait cycle count of a healthy individual. Analysis using the S-N curves showed that the screw could withstand approximately 1,519E+07 cycles at a stress of 441 MPa. Given this accumulated stress, fatigue failure was predicted to occur within approximately 38 months.

Case 2: Osteointegration Phase

As bone growth progressed into the implant, adhesion to the sacrum substantially reduced the load on the screws. The von Mises stress of the implant decreased to 12.6 MPa (Fig. 6D), indicating a marked improvement in overall implant stability. Stress on the left pelvic cortical bone, where the pelvic screws were anchored, dropped to 14.7 MPa (Fig. 6F). Most importantly, stress on the pelvic screws during the osteointegration phase was markedly reduced to 49.9 MPa (Fig. 6E). At these stress levels, fatigue life predictions based on the S-N curve indicate that screw fractures are unlikely.

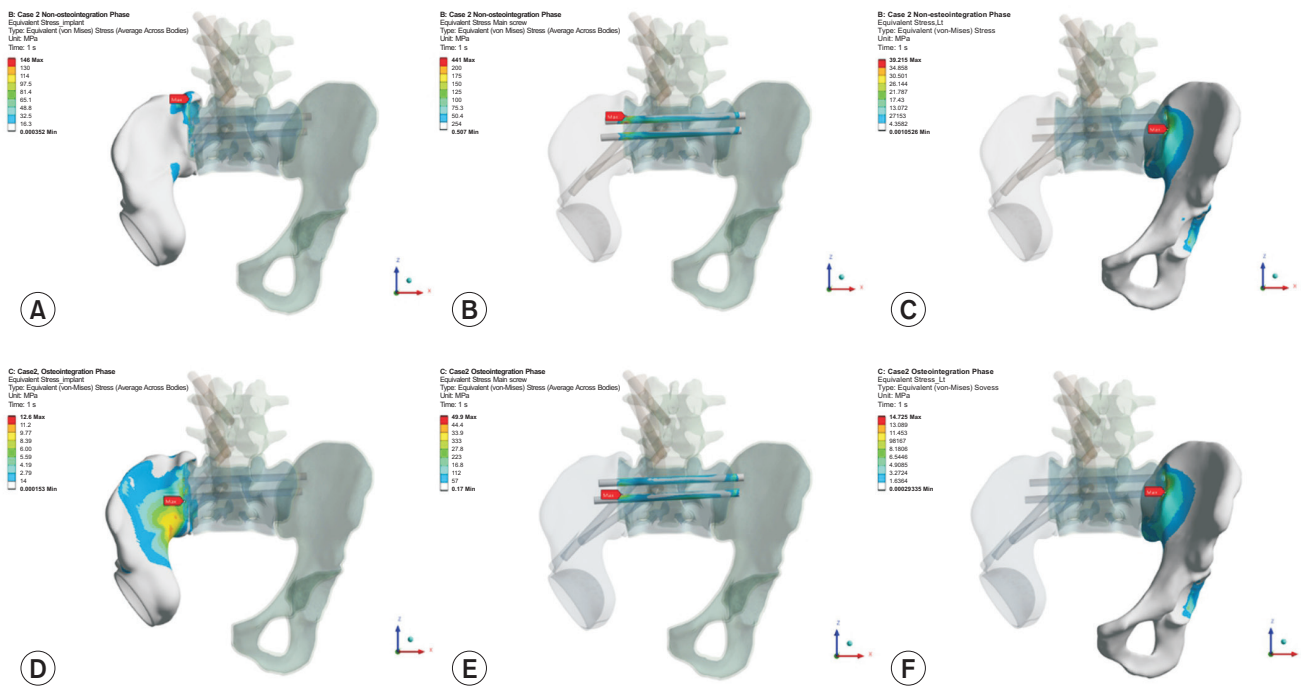

Fig. 6. Von Mises (VM) stress for case 2 during the non-osteointegration phase (A-C) and the osteointegration phase (D-F). Non-osteointegration phase, VM stress of the pelvic implant (A), main screws (B), and contralateral pelvic bone (C). Osteointegration phase, VM stress of the pelvic implant (D), main screws (E), and contralateral pelvic bone (F).

DISCUSSION

This study demonstrated the feasibility of using this method in anatomically complex and clinically demanding areas by applying the suggested FEA flow to the pelvic region. The results of this pelvis case study highlight the usefulness of the method for optimizing implant design and fixation strategies and support its use in different anatomical settings where thorough preoperative testing is not feasible.

The study was divided into non-osteointegration and osteointegration phases to evaluate the stability of implant fixation in the 2 patients and systematically analyze biomechanical problems that may occur in each phase. In the non-osteointegration phase, the short screw used for the first patient was anchored directly to the cancellous bone, which led to a high risk of pull-out. The lack of cortical bone around the cancellous bone made it difficult to achieve stable implant fixation. This challenge was confirmed during the patient's surgery, as the short screws failed to anchor properly in the cancellous bone, resulting in pull-out. In contrast, using long screws that reached the cortical bone in the second patient minimized the risk of screw pull-out. However, the analysis predicted that the cumulative fatigue load from continuous stress could cause screw fractures at 38 months after surgery. As anticipated, the long screws in the second patient fractured at 27 months after surgery, aligning closely with the predictions of the FEA model.

The osteointegration phase analysis evaluated screw and implant durability once osteointegration had formed between the implant and pelvic bone. Notably, the fatigue load on the screw reduced after successful osteointegration, lowering the risk of pelvic screw fracture. These results emphasize the importance of osteointegration in ensuring the long-term stability of the implants and screws. Therefore, patients should avoid activities that could affect implant stability and screw fixation during rehabilitation.

Our findings also prompted a reconsideration of the need for spinal fixation. A comparison between cases with and without spinal fixation showed minimal differences in the pelvic screws' stress levels (441 MPa and 453 MPa, respectively), suggesting that adding spinal fixation reduced the impact on the pelvic screws by only 3% (Fig. 7). Furthermore, the predicted fatigue life of pelvic screws with spinal fixation was 26 months, indicating that the benefits of spinal fixation may be less substantial than initially expected. Given the surgical burden and risk of infection associated with spinal fixation, the decision to perform this procedure should be carefully considered based on the patient's overall clinical condition and expected benefits.

Additionally, adjusting the screw length was proposed. Shortening the screw length may be preferable in cases in which spinal fixation is not required because of potential risks associated with longer screws that reach the far cortex, such as damage to nearby nerves and blood vessels. However, if the near cortex were included, it would be more appropriate to shorten the screw. In contrast, if neither the near cortex nor spinal fixation is used, relying solely on the cancellous bone would be insufficient because of the high risk of pull-out. Therefore, selecting an appropriate screw length and fixation method is crucial.

In the present study, bone-implant union failed in the second patient despite a postoperative period of 27 months, as evidenced by screw failure that would likely not have occurred had union been achieved. The patient received intensive chemotherapy, including doxorubicin, before and after surgery for osteosarcoma, which appears to have been the primary factor impairing bone healing.[25,26] The patient began ambulation with a walker approximately 2 weeks postoperatively and continued with crutches for 6 months during residual chemotherapy. After completing chemotherapy, the patient was pain-free during ambulation and radiologically stable, allowing full weight bearing. In cases where postoperative chemotherapy is inevitable—particularly if the bone-to-implant fusion area is small

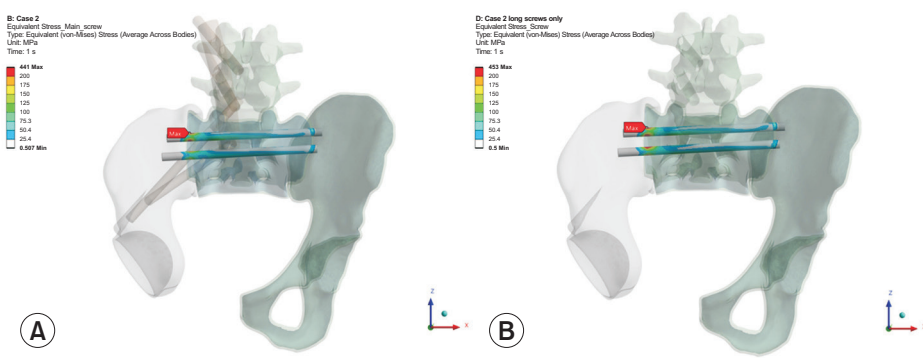

Fig. 7. Comparison between Von Mises stress of main screws with additional spinal fixation (A) and without spinal fixation (B).

relative to implant size or expected load—rehabilitation should be approached with heightened caution.

This study had some limitations. First, the models used in the simulation were simplified, excluding the internal lattice structure of the implant, and only a solid model was constructed. This simplification may have resulted in overestimating material stiffness. Additionally, data used to predict fatigue life were based on the mean number of daily steps taken by patients with hip arthroplasty, as referenced in existing literature. Consequently, these values may not fully reflect the daily activity levels of the individual patients. Nevertheless, a figure of approximately 10,000 cycles daily provides a reasonable approximation of the compressive forces applied to the spine during routine activities, such as sitting and standing, bending the waist, and going up and down stairs. Finally, the relatively low values obtained under static loading conditions are likely to be underestimated; however, the simulation results align reasonably well with the fracture patterns observed in real screws. This discrepancy was expected because the actual conditions involved dynamic and complex loading scenarios, whereas the analysis was conducted under static loading. Second, this study was a retrospective, proof-of-concept analysis that was intentionally enriched for adverse outcomes to determine whether our FEA workflow could reproduce and predict clinically observed failures. Because we did not apply the workflow to consecutive or uncomplicated reconstructions, this report cannot provide estimates of diagnostic performance such as sensitivity, specificity, or false-positive rate (i.e., cases wherein FEA would predict failure but the patient had an uneventful clinical course). Future research will apply the FEA workflow prospectively to a consecutive series of patients (with blinded predictions) to quantify predictive accuracy and to refine model thresholds for clinical decision making.

The FEA-based analysis flow presented in this study is designed for application in the iterative redesign process of 3D-printed implants and is useful for predicting and validating the analysis flow at different sites and fixation methods. In particular, preoperative evaluation of different sites can be a practical guide for surgeons to reconsider the surgical approach and offer an essential alternative in situations where it is impractical to validate all implants before surgery fully. In the future, it is expected that FEA flow can be added between the design and printing processes to shorten the time required to increase real-time applicability. This study's methodology can be extended to accommodate a range of clinical conditions.

In conclusion, this study demonstrated that the FEA method can be effectively applied in evaluating patient-customized 3D-printed implants. Screw-fixation stability, which directly influences screw pull-out and fracture, is critical in implant surgery and emphasizes the importance of optimizing implant design and fixation methods. This study also showed that the timing of screw-fatigue failure can be approximately predicted and can contribute to improved implant design and surgical techniques. The FEA methodology proposed in this study provides a practical solution for preoperative planning and iterative implant design, potentially reducing the need for extensive physical testing while accommodating a range of clinical conditions. To enable the application of 3D-printed implants across various sites, future studies should incorporate sophisticated simulations that reflect various clinical scenarios, furthering the applicability of FEA in preoperative planning.

CONFLICT OF INTEREST

No potential conflict of interest relevant to this article was reported.

ACKNOWLEDGEMENTS

This study was supported by Soon Bo Baek (TAE SUNG S&E Company) and National Research Foundation of Korea grant funded by the Korea government (MSIT) (No. 2023R1A2C200341711).

ORCID

Suyeon Lee https://orcid.org/0009-0008-1735-0089
Hyenmin Park https://orcid.org/0009-0005-5665-6572
Hyun Guy Kang https://orcid.org/0000-0003-1994-6990
June Hyuk Kim https://orcid.org/0000-0002-8899-5342
Im Doo Jung https://orcid.org/0000-0003-0883-1848
Jong Woong Park https://orcid.org/0000-0002-8044-7624

REFERENCES

1. Kang HG. Clinical atlas of 3D printing bone reconstruction. 1st ed. Springer Verlag; 2021.
2. Liang H, Ji T, Zhang Y, Wang Y, Guo W. Reconstruction with 3D-printed pelvic endoprostheses after resection of a

pelvic tumour. Bone Joint J. 2017;99(2):267-75.

3. Imanishi J, Choong PF. Three-dimensional printed calcaneal prosthesis following total calcanectomy. Int J Surg Case Rep. 2015;10:83-7.
4. Wong KC, Kumta SM, Geel NV, Demol J. One-step reconstruction with a 3D-printed, biomechanically evaluated custom implant after complex pelvic tumor resection. Comput Aided Surg. 2015;20(1):14-23.
5. Fan H, Fu J, Li X, et al. Implantation of customized 3-D printed titanium prosthesis in limb salvage surgery: a case series and review of the literature. World J Surg Oncol. 2015; 13:308.
6. Yan M, Huang J, Ding M, Wang J, Song D. 3D-printed model is a useful addition in orthopedic resident education for the understanding of tibial plateau fractures. Sci Rep. 2024; 14(1):24880.
7. Park JW, Kang HG, Kim JH, Kim HS. The application of 3D-printing technology in pelvic bone tumor surgery. J Orthop Sci. 2021;26(2):276-83.
8. Zhu D, Fu J, Wang L, Guo Z, Wang Z, Fan H. Reconstruction with customized, 3D-printed prosthesis after resection of periacetabular Ewing's sarcoma in children using "triradiate cartilage-based" surgical strategy: a technical note. J Orthop Translat. 2021;28:108-17.
9. Li Z, Wang C, Li C, et al. What we have achieved in the design of 3D printed metal implants for application in orthopedics? Personal experience and review. RPJ. 2018;24(8): 1365-79.
10. Brouwer de Koning SG, de Winter N, Moosabeiki V, et al. Design considerations for patient-specific bone fixation plates: a literature review. Med Biol Eng Comput. 2023; 61(12):3233-52.
11. Yan L, Lim JL, Lee JW, Tia CS, O'Neill GK, Chong DY. Finite element analysis of bone and implant stresses for customized 3D-printed orthopaedic implants in fracture fixation. Med Biol Eng Comput. 2020;58(5):921-31.
12. Huang S, Ji T, Guo W. Biomechanical comparison of a 3D-printed sacrum prosthesis versus rod-screw systems for reconstruction after total sacrectomy: a finite element analysis. Clin Biomech (Bristol). 2019;70:203-8.
13. Wu C, Zeng B, Deng J, et al. Finite element analysis and transiliac-transsacral screw fixation for posterior pelvic ring with sacrum dysplasia. Orthop Surg. 2023;15(1):337-46.
14. Yao Y, Mo Z, Wu G, et al. A personalized 3D-printed plate for tibiotalocalcaneal arthrodesis: design, fabrication, biomechanical evaluation and postoperative assessment. Comput Biol Med. 2021;133:104368.
15. Yañez R, Silvestre R, Roby M, et al. Finite element graft stress for anteromedial portal, transtibial, and hybrid transtibial femoral drillings under anterior translation and medial rotation: an exploratory study. Sci Rep. 2024;14(1):11922.
16. Hamidi S, Khosravifard A, Hematiyan MR, Dehghani J. A comparative mechanical study of two types of femur bone implant using the finite element method. Int J Numer Method Biomed Eng. 2021;37(6):e3459.
17. Gefen A. Optimizing the biomechanical compatibility of orthopedic screws for bone fracture fixation. Med Eng Phys. 2002;24(5):337-47.
18. Zhang QH, Tan SH, Chou SM. Investigation of fixation screw pull-out strength on human spine. J Biomech. 2004; 37(4):479-85.
19. Izzawati B, Daud R, Rojan A, et al. The effect of bone healing condition on the stress of screw fixation in orthotropic femur bone for fracture stabilization. Mater Today Proc. 2019;16:2160-9.
20. Zhao Y, Zhang S, Sun T, et al. Mechanical comparison between lengthened and short sacroiliac screws in sacral fracture fixation: a finite element analysis. Orthop Traumatol Surg Res. 2013;99(5):601-6.
21. Bianco RJ, Arnoux PJ, Wagnac E, Mac-Thiong JM, Aubin CÉ. Minimizing pedicle screw pullout risks: a detailed biomechanical analysis of screw design and placement. Clin Spine Surg. 2017;30(3):E226-32.
22. Belan J, Kuchariková L, Tillová E, Chalupová M. Three-point bending fatigue test of tial6v4 titanium alloy at room temperature. Adv Mater Sci Eng. 2019;2019:1-11.
23. Miner MA. Cumulative damage in fatigue. J Appl Mech. 1945;12:A159-64.
24. Schmalzried TP, Szuszczewicz ES, Northfield MR, et al. Quantitative assessment of walking activity after total hip or knee replacement. J Bone Joint Surg Am. 1998;80(1):54-9.
25. Mumith A, Coathup M, Edwards TC, Gikas P, Aston W, Blunn G. Multidrug chemotherapy causes early radiological signs of loosening in distal femoral replacements. Bone Joint Res. 2020;9(7):333-40.
26. Virolainen P, Inoue N, Nagao M, Frassica FJ, Chao EY. The effect of multidrug chemotherapy on bone graft augmented prosthesis fixation. J Orthop Res. 2005;23(4):795-801.